

Double-layered passivation film structure of $\text{Al}_2\text{O}_3/\text{SiN}_x$ for high mobility oxide thin film transistors

Sang-Hee Ko Park, Min-Ki Ryu, Himchan Oh, Chi-Sun Hwang, Jae-Hong Jeon, and Sung-Min Yoon

Citation: *Journal of Vacuum Science & Technology B* **31**, 020601 (2013); doi: 10.1116/1.4789423

View online: <https://doi.org/10.1116/1.4789423>

View Table of Contents: <https://avs.scitation.org/toc/jvb/31/2>

Published by the [American Vacuum Society](#)

ARTICLES YOU MAY BE INTERESTED IN

High-mobility thin-film transistor with amorphous InGaZnO_4 channel fabricated by room temperature rf-magnetron sputtering

Applied Physics Letters **89**, 112123 (2006); <https://doi.org/10.1063/1.2353811>

Origin of threshold voltage instability in indium-gallium-zinc oxide thin film transistors

Applied Physics Letters **93**, 123508 (2008); <https://doi.org/10.1063/1.2990657>

Electronic transport properties of amorphous indium-gallium-zinc oxide semiconductor upon exposure to water

Applied Physics Letters **92**, 072104 (2008); <https://doi.org/10.1063/1.2838380>

Hydrogen passivation of electron trap in amorphous In-Ga-Zn-O thin-film transistors

Applied Physics Letters **103**, 202114 (2013); <https://doi.org/10.1063/1.4832076>

Origins of threshold voltage shifts in room-temperature deposited and annealed $\alpha\text{-In-Ga-Zn-O}$ thin-film transistors

Applied Physics Letters **95**, 013502 (2009); <https://doi.org/10.1063/1.3159831>

Improvements in the device characteristics of amorphous indium gallium zinc oxide thin-film transistors by Ar plasma treatment

Applied Physics Letters **90**, 262106 (2007); <https://doi.org/10.1063/1.2753107>



NEW

AVS Quantum Science
A high impact interdisciplinary journal for **ALL** quantum science

ACCEPTING SUBMISSIONS

The banner features the AVS Publishing logo on the left, the journal title and tagline in the center, and a red button with the text 'ACCEPTING SUBMISSIONS' on the right. The background is decorated with various quantum science icons such as a triangle with a circle inside, a cat face, a brain, a signal wave, and an atom.

LETTERS

Double-layered passivation film structure of $\text{Al}_2\text{O}_3/\text{SiN}_x$ for high mobility oxide thin film transistors

Sang-Hee Ko Park,^{a)} Min-Ki Ryu, Himchan Oh, and Chi-Sun Hwang
*Oxide TFT Research Team, Electronics and Telecommunications Research Institute, Yuseong,
Daejeon 305-700, Korea*

Jae-Hong Jeon
*Telecommunications and Computer Engineering, Korea Aerospace University, Goyang,
Gyeonggi-do 412-791, Korea*

Sung-Min Yoon^{b)}
*Department of Advanced Materials Engineering for Information and Electronics, Kyung Hee University,
Yongin, Gyeonggi-do 446-701, Korea*

(Received 22 October 2012; accepted 10 January 2013; published 24 January 2013)

The optimization of the passivation process for oxide thin film transistors with high carrier mobility was investigated. Hydrogen incorporation into oxide channels during the deposition of SiN_x could degrade device stability and uniformity, especially for high-mobility devices. A novel double-layered passivation film structure composed of $\text{Al}_2\text{O}_3/\text{SiN}_x$ was proposed, in which thin and dense Al_2O_3 film prepared by atomic layer deposition was introduced underneath the SiN_x layer. In-Ga-Zn-O TFT passivated with the proposed double-layered films showed no significant negative shift in turn-on voltage, even after passivation. The field-effect mobility and subthreshold swing were typically measured as $27.7 \text{ cm}^2 \text{ V}^{-1} \text{ s}^{-1}$ and 0.11 V/dec , respectively. Hydrogen doping was effectively protected by the introduction of Al_2O_3 as thin as 15 nm. © 2013 American Vacuum Society. [<http://dx.doi.org/10.1116/1.4789423>]

I. INTRODUCTION

Oxide semiconductor thin film transistors (TFTs) have attracted attention as a promising backplane device for large-area and high-resolution flat-panel displays (FPD).¹⁻³ Amorphous phase In-Ga-Zn-O (IGZO) is one of the most typical oxide TFTs compositions due to its relatively high field-effect mobility (μ_{FE}) and superior uniformity.^{4,5} LG Display has released a 55-in. full-high-definition (FHD) organic light-emitting diode (OLED) TV employing an IGZO oxide TFT active matrix (AM).⁶ During the initial stage of development, the μ_{FE} of the oxide TFT, which is approximately $10 \text{ cm}^2 \text{ V}^{-1} \text{ s}^{-1}$ for IGZO TFTs, was considered sufficient for state-of-the-art ultra-definition (UD) TV panels and higher-resolution mobile displays. However, recent trends and situations in the FPD industry have led to the rapid change to new phases, such as 4K8K panels and 3D displays. As a result, further improvements in μ_{FE} and its stability of the oxide TFT are urgently required to broaden the potential applications. To drive those FPD panels and integrate peripheral driving circuitry, the oxide TFTs with μ_{FE} higher than $30 \text{ cm}^2 \text{ V}^{-1} \text{ s}^{-1}$ are required. In viewpoints of oxide active channels, the methodologies to enhance the μ_{FE} can be roughly classified as follows: (1) modification of

the composition of IGZO in terms of its atomic ratio has produced large values of μ_{FE} , ranging from 24.2 to $46 \text{ cm}^2 \text{ V}^{-1} \text{ s}^{-1}$;⁷⁻⁹ (2) new compositions, such as Zn-In-Sn-O,¹⁰⁻¹² Al-Sn-Zn-In-O,¹³ and In-Ga-O,^{14,15} have been reported to show μ_{FE} values of 51.7 , 31.9 , and $43 \text{ cm}^2 \text{ V}^{-1} \text{ s}^{-1}$, respectively; and (3) double-stacked active layers composed of high- and low-density carrier layers were also proposed as a promising approach.^{16,17} A common strategy for high mobility oxide TFT is increasing the carrier amount within the active channel layer.¹⁸ It is important to note that the prescriptions employed for the high μ_{FE} should not degrade device stability and uniformity. A broad run-to-run or device-to-device variations in important device parameters, including the threshold voltage (V_{th}), can have fatal effects on the integration of AM-FPD's due to the narrow process window. The detrimental variation in V_{th} is closely related to the passivation process, which is generally performed to protect the oxide TFTs from the ambient. Al_2O_3 film deposited by atomic layer deposition (ALD) has exhibited excellent passivation capabilities for realizing the stable high-mobility oxide TFTs,^{13,19} which has also been successfully demonstrated as good gate insulator and/or protection layer for the oxide active channel by ETRI (Korea).^{20,21} Sony (Japan) reported the high-mobility oxide TFTs passivated with the Al_2O_3 film deposited by reactive DC sputtering method, which was selected in viewpoint of the process compatibility to large panel size.^{9,12} Spin-coated epoxy-based SU-8 resist was also

^{a)}Electronic mail: shkp@etri.re.kr

^{b)}Electronic mail: sungmin@khu.ac.kr

proposed as a potential passivation layer, with which a very stable IGZO TFT with a mobility of $61 \text{ cm}^2 \text{ V}^{-1} \text{ s}^{-1}$ was obtained.²² Some fabrication techniques have employed an etch-stop layer (ESL) of SiO_x prepared by plasma enhanced chemical vapor deposition (PECVD).^{4,10} Although SiN_x films grown by PECVD have been employed for the poly-silicon and organic TFTs owing to its excellent barrier properties,^{23,24} there hardly been reports on the high-mobility oxide TFTs passivated with SiN_x film. In this work, the importance of the passivation process producing an oxide TFT with higher μ_{FE} and device stability were investigated. In order to optimize the device structure of the high-mobility IGZO TFT, a double-layered passivation film structure of ALD- Al_2O_3 /PECVD- SiN_x and a PL-incorporated bottom-gate coplanar gate configuration was proposed. This simple fabrication process was confirmed to be very promising for obtaining a stable oxide TFT with a high μ_{FE} .

II. EXPERIMENT

A bottom gate IGZO TFT with an ESL was first fabricated as a controlled device in order to confirm the effect of the SiN_x passivation layer on the characteristics of the fabricated TFT. A 150-nm-thick molybdenum-titanium (Mo-Ti) layer patterned on a glass substrate was used as a bottom gate electrode. For a gate insulator, SiO_2 (200 nm) was deposited by PECVD using SiH_4 and N_2O at 380°C . α -IGZO film with a thickness of 25 nm was prepared by RF sputtering using a single IGZO (In:Ga:Zn = 1:1:1 atomic ratio) target at room temperature, followed by deposition of a SiO_2 (100 nm) ESL by PECVD at 300°C . The SiO_2 ESL and IGZO active channel were patterned by dry and wet etching processes, respectively. Mo-Ti source and drain (S/D) electrodes (150 nm) were deposited by sputtering and patterned by wet chemical etching. The controlled device was passivated by $\text{SiO}_2/\text{SiN}_x$ double-layered passivation films, in which SiO_2 (150 nm) and SiN_x (150 nm) layers were prepared by PECVD at a temperature of 300°C . A cross-sectional schematic diagram of the controlled device is shown in Fig. 1(a).

The proposed device was fabricated as a bottom-gate bottom-contact (coplanar) structure with a PL of Al_2O_3 substituting for the SiO_2 ESL, as schematically shown in Fig. 2(a). Indium tin oxide (ITO, 150 nm) was patterned on a glass substrate as a gate electrode. After Al_2O_3 (185 nm) was deposited by ALD as the gate insulator using an Al precursor of trimethylaluminum and water vapor at a temperature of 200°C , an ITO film (150 nm) was deposited by sputtering and was patterned into S/D electrodes. An α -IGZO (30 nm) active layer and an Al_2O_3 (9 nm) PL were successively prepared by RF sputtering and ALD processes, respectively. In this fabrication, the composition of IGZO was controlled to produce high mobility. The active patterns were defined by conventional photolithography and patterned by wet chemical etching using diluted hydrofluoric acid (HF) chemistry. The proposed device was passivated by double-layered films of $\text{Al}_2\text{O}_3/\text{SiN}_x$, in which Al_2O_3 and SiN_x (200 nm) layers were prepared by ALD at 200°C and PECVD at 300°C , respectively. The film

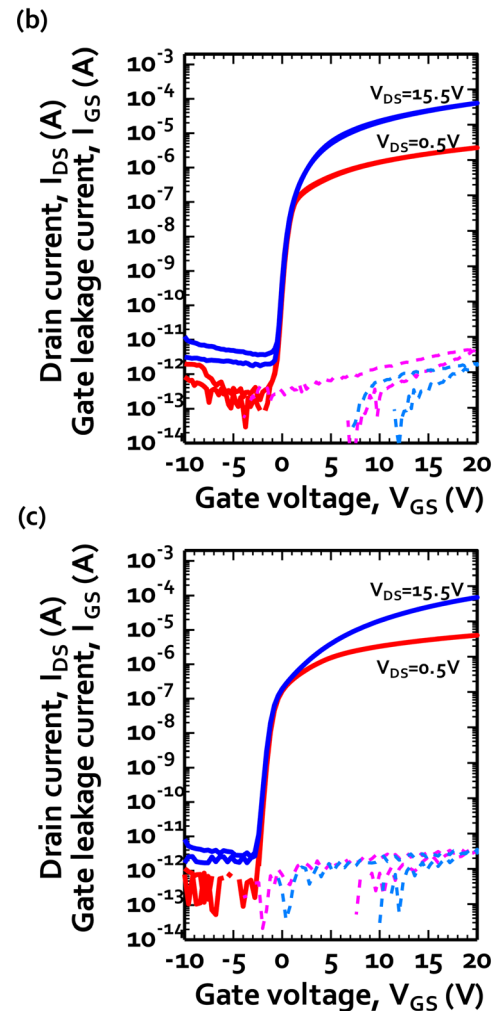
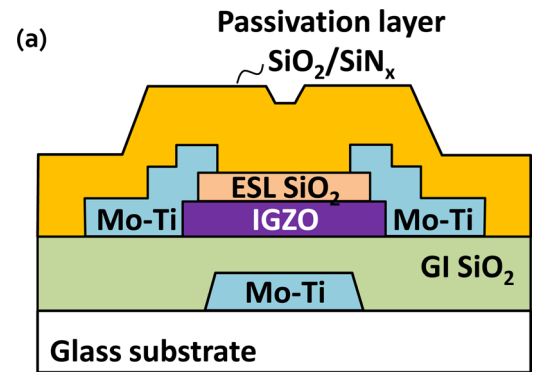


FIG. 1. (Color online) (a) Schematic cross-sectional diagrams of the controlled device with an etch-stop layer of SiO_2 and bottom-gate configuration that was passivated using a double-layered structure of $\text{SiO}_2/\text{SiN}_x$. I_{DS} - V_{GS} transfer characteristics of the fabricated IGZO TFTs (b) before and (c) after the passivation process. The gate width and length of the evaluated device were 40 and 20 μm , respectively.

thickness of the Al_2O_3 layer was controlled by changing the number of ALD cycles from 100 to 400.

The electrical characteristics of the fabricated IGZO TFTs were evaluated using a semiconductor parameter analyzer (Agilent B1500A) in a dark box at room temperature. All devices were thermally annealed at 250°C for 2 h before electrical evaluation.

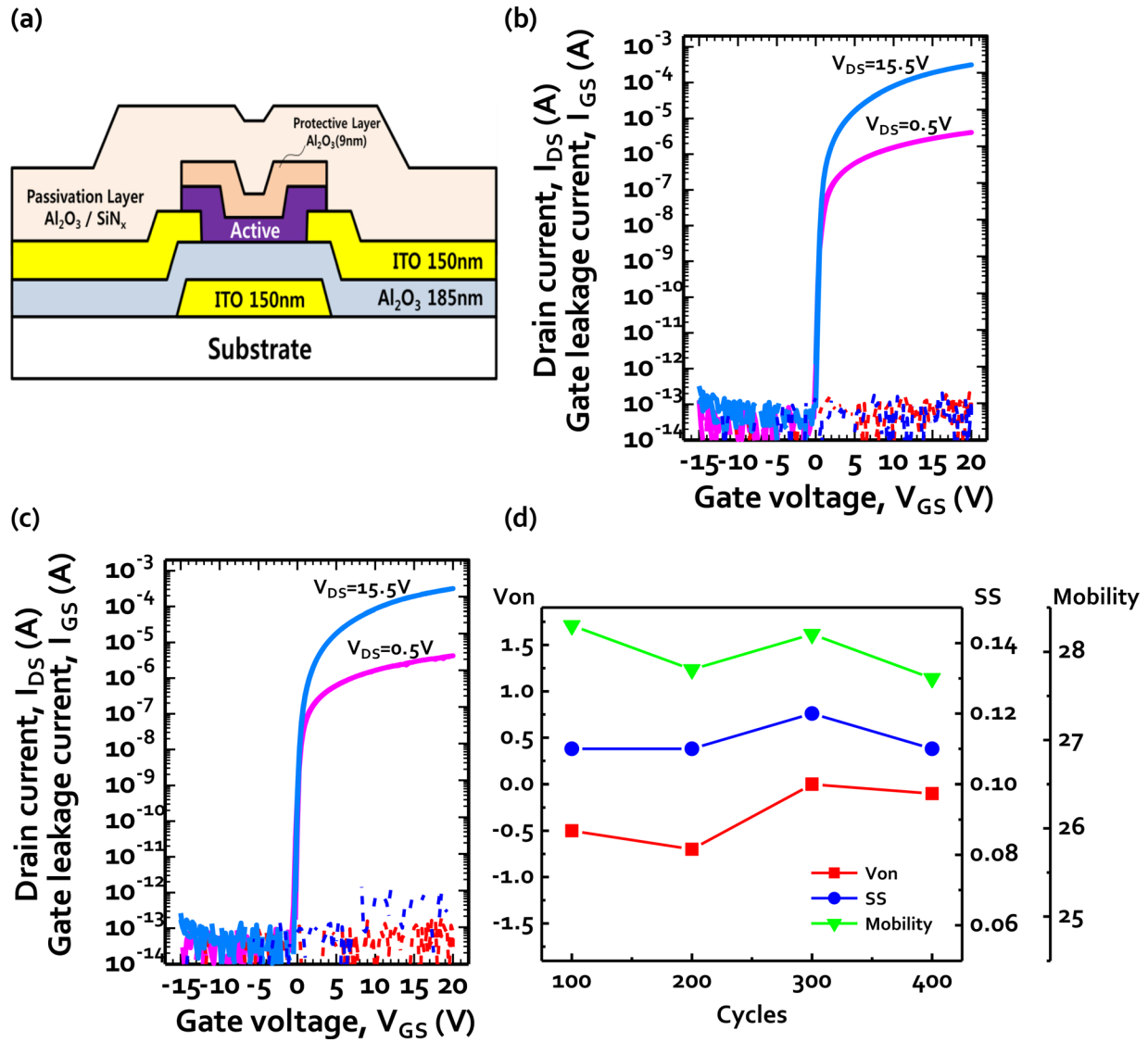


FIG. 2. (Color online) (a) Schematic cross-sectional diagrams of the proposed device passivated by double-layered structure of Al₂O₃/SiN_x. The I_{DS} - V_{GS} characteristics of the IGZO TFTs when the number of ALD cycles of the Al₂O₃ were varied: (b) 400 and (c) 100 cycles. (d) Summary of the device parameters of the μ_{FE} , V_{on} , SS, and their variations as a function of the number of ALD cycles.

III. RESULTS AND DISCUSSION

Figures 1(b) and 1(c) show the drain current (I_{DS})-gate voltage (V_{GS}) transfer characteristics of the controlled device before and after the passivation process, respectively. The measurements were successively performed at drain voltages (V_{DS}) of 0.5 and 15.5 V at forward and reverse sweeps of V_{GS} for each device with a gate width (W) of 40 and length (L) of 20 μm . Before the passivation process, the turn-on voltage (V_{on}) of the TFT was measured at a V_{GS} of approximately 0 V. The transfer curves exhibited good behaviors of sufficiently low off-current and negligible hysteresis in the trace of I_{DS} . However, the V_{on} of the passivated device showed a drastic negative shift without the degradation of any other properties of the device. The drawback of the PECVD SiN_x passivation layer is that hydrogen could be incorporated into the active channel layer during the deposition process. Hydrogen incorporation induces a doping effect

on the IGZO channel and abruptly increases the carrier concentration within the channel. Some TFTs fabricated on the same substrate showed fully conductive behavior for the evaluated V_{GS} range (not shown here). This result suggests that hydrogen incorporation during PECVD deposition degrades the device-to-device uniformity and causes an undesirable doping effect. Unlike SiN_x, during the deposition of SiO₂, a strong oxidation agent N₂O can continuously supply oxygen such that oxygen vacancies can be eliminated, even during a PECVD process using a hydrogen containing SiH₄ source. Therefore, passivation using PECVD SiO₂ can be a promising alternative for preventing hydrogen incorporation into the semiconducting channel of oxide TFT.²⁵ Eventually, the SiN_x cannot be directly prepared on the active channel layer of the oxide TFT, even though the barrier property of SiN_x is much superior to that of SiO₂. The main purpose of using the double-layered passivation SiO₂/SiN_x film for the controlled device was to confirm the

feasibility of its use in terms of its high impermeability to ambient (SiN_x) and its strong resistance to hydrogen doping (SiO_2). However, hydrogen incorporation could not be perfectly suppressed despite the introduction of an SiO_2 ESL and the use of the first passivation layer of SiO_2 underneath the second passivation layer of SiN_x .

It is interesting to investigate the relationship between the degree of negative shift in V_{on} (or V_{th}) and the carrier concentration of the active channel when a given amount of donor is doped into the oxide channel. Figure 3 shows the simulated results of the variations in the transfer characteristics by donor doping when the carrier concentration of the channel layer was varied. An ATLAS device simulator (Silvaco) was employed for these simulations, and the important material parameters required to electrically model the device were adjusted. As shown in Fig. 3(a), while a certain amount of donor doping did not significantly causes a negative shift in V_{on} in the device with a relatively low carrier concentration, the device with a higher carrier concentration experienced a larger negative shift. Since the carrier amount within the channel increased with the film thickness of the channel layer, the shifting rate of the transfer curve accelerated when the film thickness increased from 25 [Fig. 3(a)] to 50 nm

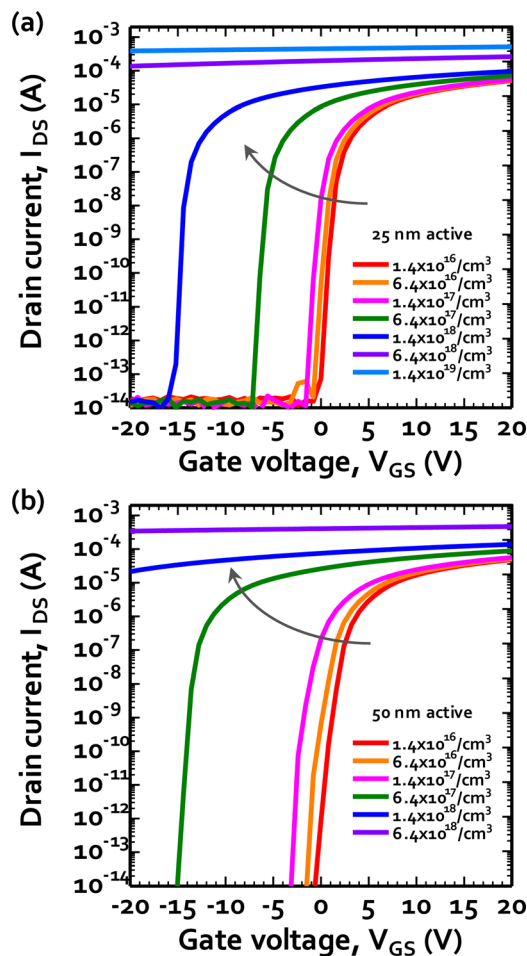


FIG. 3. (Color online) Simulation results of the transfer characteristics of TFTs with active layer thicknesses of (a) 25 and (b) 50 nm. The variations in characteristics were estimated for active channels with different carrier concentrations when a certain amount of donor was doped into the active channel.

[Fig. 3(b)]. Consequently, additional carriers incorporated into the active channel by hydrogen doping could be ignored for an oxide TFT with a moderate carrier density and moderate mobility. However, we have to remind that the transfer characteristics of the oxide TFT with a high carrier density and higher value of mobility could be very sensitive to being affected (negatively shifted) even by the incorporation of a small amount of hydrogen. These estimates indicate that the importance of the passivation process for the realization of a stable high-mobility oxide TFT cannot be overemphasized.

There was further supporting evidence to show the effect of hydrogen incorporation into oxide semiconducting thin films on their electrical properties. Figures 4(a) and 4(b) show the variations in sheet resistance (R_s) measured at the forward and reverse sweeps in temperature for the ZnO films deposited on the thermal oxide and PECVD- SiO_2 layers, respectively. As shown in Fig. 4(a), the R_s decreased and increased with increasing and decreasing temperature, respectively, over 50–350 °C, indicating that the prepared ZnO film is capable of semiconducting behavior. Furthermore, the temperature dependence was nearly reversible, and there was no marked variation among measured samples. Alternatively, the R_s values of the ZnO films prepared on the PECVD- SiO_2 layer exhibited large decreases with

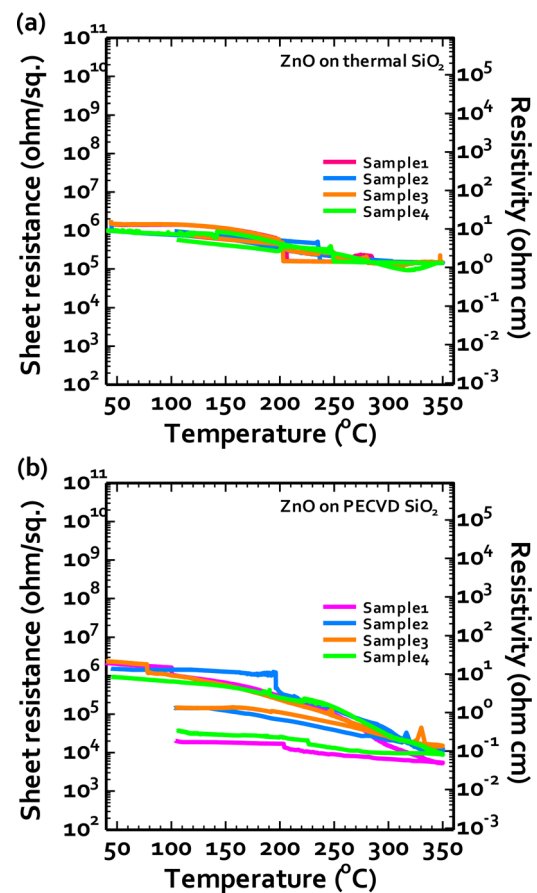


FIG. 4. (Color online) Variation in sheet resistance of ZnO thin film deposited on (a) thermal oxide and (b) PECVD- SiO_2 , which was measured *in situ* with temperature in both forward and reverse directions. The measurements were repeated for four different samples for each condition in order to examine the uniformity and reproducibility of the obtained data.

increased temperature and did not return to their initial values, even when the temperature was lowered. The residual hydrogen in the PECVD SiO₂ layer may be incorporated into the ZnO film at an elevated temperature and increases the carrier concentration and electrical conductivity of the ZnO surface. The large variation in the final R_s values among the measured samples indicate that this kind of donor doping may be uncontrollable and eventually degrade the run-to-run uniformity of the oxide TFT.

Based on these investigations and the obtained results, a double-layered Al₂O₃/SiN_x was proposed as a novel passivation film structure for a high-mobility oxide TFT, as shown in Fig. 2(a). This combined structure is designed to exploit the high resistance of the ALD-grown thin Al₂O₃ (the first layer) against undesirable hydrogen doping and the high barrier property of the PECVD-SiN_x (the second layer) from the ambient. The carrier concentration and Hall mobility of the IGZO active layer with modified composition were approximately $1.4 \times 10^{18} \text{ cm}^{-3}$ and $15 \text{ cm}^2 \text{ V}^{-1} \text{ s}^{-1}$ before the formation of PL. Figure 2(b) shows the I_{DS} - V_{GS} characteristics of the fabricated device when the second passivation layer of Al₂O₃ was prepared by performing 400 cycles in the ALD process. The μ_{FE} , V_{on} , and subthreshold swing (SS) were measured to be approximately $27.7 \text{ cm}^2 \text{ V}^{-1} \text{ s}^{-1}$, -0.10 V , and 0.11 V/dec , respectively. The proposed device exhibited excellent TFT behaviors, including high μ_{FE} and low off-current. These characteristics were confirmed to show no marked variation or degradation, even when the number of ALD cycles was reduced to 100, which corresponded to a thickness of approximately 15 nm, as shown in Fig. 2(c). Figure 2(d) summarizes the obtained device parameters of μ_{FE} , V_{on} , SS, and their variations as a function of the number of cycles (film thickness) during the ALD process for the Al₂O₃ layer. The μ_{FE} values were higher than $27 \text{ cm}^2 \text{ V}^{-1} \text{ s}^{-1}$ and were all within a small range from 27.7 to $28.3 \text{ cm}^2 \text{ V}^{-1} \text{ s}^{-1}$. It was also impressive that the V_{on} values did not shift in the negative direction, even after the final SiN_x passivation process and that their values were in the range of -0.7 to 0 V . This result clearly suggests that the introduction of Al₂O₃ as thin as 15 nm can effectively protect against hydrogen incorporation during the SiN_x deposition process. This is the first demonstration on the methodologies with which we can exploit the excellent barrier properties of SiN_x film without degrading the operational stability of oxide TFTs, although there have been some reports on the process providing the function of effective passivation for the oxide TFTs so far.^{9,10,12,13,22} The bias temperature stability of the proposed device was also examined. Especially for the high-mobility oxide TFTs, both processes of active channel composition and passivation layer structure should comprehensively be controlled in order to effectively improve the device stability. Although additional optimization will be necessary for our device, the V_{on} shift could be suppressed to be less than 0.6 V when a V_{GS} of $+20 \text{ V}$ was applied as a positive bias stress at 60°C for 10^4 s . The further investigations on the ageing effects with the evolution of time and the device stabilities under light illumination with various wavelengths would be also very important issues for the

double-layered passivation film structure proposed in this work. These characterizations are planned to be intensively investigated and analyzed in a detailed manner as our next publications.

IV. CONCLUSION

A novel double-layered passivation film structure composed of Al₂O₃/SiN_x for high-mobility oxide TFTs was proposed. In order to realize the stable characteristics and wide process margin for the oxide TFT with a higher mobility, the hydrogen doping effect should be carefully controlled during the passivation process, which is generally performed using a PECVD process with hydrogen-containing SiH₄ sources. The incorporation of hydrogen into the oxide channel caused an adverse negative shift in V_{on} (or V_{th}) after the passivation process, and the oxide channel with a higher carrier density was anticipated to be more sensitive to this effect. Consequently, passivation processes for high-mobility oxide TFT should be optimized, because devices would experience a critical degradation in its stability and uniformity even with a small amount of hydrogen incorporation. The proposed double-layered passivation films could be expected to offer both high resistance against hydrogen doping (Al₂O₃) and high barrier properties against the ambient (SiN_x). The IGZO TFT fabricated using the proposed passivation process showed excellent characteristics, including V_{on} stability after the passivation, in which μ_{FE} and SS were measured as $27.7 \text{ cm}^2 \text{ V}^{-1} \text{ s}^{-1}$ and 0.11 V/dec , respectively. It was also confirmed that hydrogen incorporation can be effectively prevented by the introduction of Al₂O₃ as thin as 15 nm. Although future investigations on the bias-stress stability, light-stress stability, and ageing effect will provide more detailed insights on the designed process and structure, the double-layered passivation film structure proposed in this work can be concluded to present a potential strategy for developing and optimizing the fabrication processes of higher-mobility oxide TFTs as a promising driving force to next-generation FPD industries.

ACKNOWLEDGMENT

This work was supported by the Industrial Strategic Technology Development program (Project number 10035225, Development of Core Technology for High Performance AMOLED on Plastic) funded by MKE/KEIT.

¹H. Ohara *et al.*, *Jpn. J. Appl. Phys.* **49**, 03CD02 (2010).

²H. H. Lu, H. C. Ting, T. H. Shih, C. Y. Chen, C. S. Chuang, and Y. Lin, *SID Int. Symp. Digest Tech. Papers* **2010**, 1136.

³T. Osada, K. Akimoto, T. Sato, M. Ikeda, M. Tsubuku, J. Sakata, J. Koyama, T. Serikawa, and S. Yamazaki, *Jpn. J. Appl. Phys.* **49**, 03CC02 (2010).

⁴K. Nomura, H. Ohta, A. Takagi, T. Kamiya, M. Hirano, and H. Hosono, *Nature* **432**, 488 (2004).

⁵E. Fortunato, P. Barquinha, and R. Martins, *Adv. Mat.* **24**, 2945 (2012).

⁶C. W. Han, K. M. Kim, S. J. Bae, H. S. Choi, J. M. Lee, T. S. Kim, Y. H. Tak, S. Y. Cha, and B. C. Ahn, *SID Int. Symp. Digest Tech. Papers* **2012**, 279.

⁷P. Barquinha, L. Pereira, G. Gonçalves, R. Martins, and E. Fortunato, *Electrochem. Solid-State Lett.* **11**, H248 (2008).

- ⁸M. Kim, J. H. Jeong, H. J. Lee, T. K. Ahn, H. S. Shin, J. S. Park, J. K. Jeong, Y. G. Mo, and H. D. Kim, *Appl. Phys. Lett.* **90**, 212114 (2007).
- ⁹T. Arai and T. Sasaoka, *SID Int. Symp. Digest Tech. Papers* **2011**, 710.
- ¹⁰D. Wang, C. Li, M. Furuta, S. Tomai, M. Sunagawa, M. Nishimura, E. Kawashima, M. Kasami, and K. Yano, *Proc. AM-FPD12* **2012**, 159.
- ¹¹M. K. Ryu, S. Yang, S. H. Ko Park, C. S. Hwang, and J. K. Jeong, *Appl. Phys. Lett.* **95**, 072104 (2009).
- ¹²E. Fukumoto, T. Arai, N. Morosawa, K. Tokunaga, Y. Terai, T. Fujimori, and T. Sasaoka, *J. SID* **19**, 867 (2011).
- ¹³S. Yang, D. H. Cho, M. K. Ryu, S. H. Ko Park, C. S. Hwang, J. Jang, and J. K. Jeong, *IEEE Electron Devices Lett.* **31**, 144 (2010).
- ¹⁴G. Gonçalves, P. Barquinha, L. Pereira, N. Franco, E. Alves, R. Martins, and E. Fortunato, *Electrochem. Solid-State Lett.* **13**, H20 (2010).
- ¹⁵K. Ebata, S. Tomai, Y. Tsuruma, T. Litsuka, S. Matsuzaki, and K. Yano, *Appl. Phys. Express* **5**, 011102 (2012).
- ¹⁶S. Taniguchi, M. Yokozeki, M. Ikeda, and T. Suzuki, *Jpn. J. Appl. Phys.* **50**, 04DF11 (2011).
- ¹⁷J. C. Park and H. N. Lee, *IEEE Electron Devices Lett.* **33**, 818 (2012).
- ¹⁸T. Kamiya, K. Nomura, and H. Hosono, *J. Disp. Tech.* **5**, 273 (2009).
- ¹⁹S. Yang, D. H. Cho, M. K. Ryu, S. H. Ko Park, C. S. Hwang, J. Jang, and J. K. Jeong, *Appl. Phys. Lett.* **96**, 213511 (2010).
- ²⁰W. S. Cheong *et al.*, *ETRI J.* **31**, 660 (2009).
- ²¹S. H. Ko Park *et al.*, *ETRI J.* **31**, 653 (2009).
- ²²A. Olziersky, P. Barquinha, A. Vilà, L. Pereira, G. Gonçalves, E. Fortunato, R. Martins, and J. R. Morante, *J. Appl. Phys.* **108**, 064505 (2010).
- ²³C. C. Liao, M. C. Lin, T. Y. Chiang, and T. S. Chao, *IEEE Trans. Electron Devices* **58**, 3812 (2011).
- ²⁴J. S. Meena, M. C. Chu, C. S. Wu, F. C. Chang, and F. H. Ko, *Org. Electron.* **12**, 1414 (2011).
- ²⁵K. S. Son *et al.*, *SID Int. Symp. Digest Tech. Papers* **2008**, 633.